HHS Public Access

Author manuscript

Dev Biol. Author manuscript; available in PMC 2022 September 01.

Published in final edited form as:

Dev Biol. 2021 September ; 477: 133–144. doi:10.1016/j.ydbio.2021.05.012.

Merlin and *expanded* integrate cell signaling that regulates cyst stem cell proliferation in the *Drosophila* testis niche

Bryan Johnson[1,2], **Judith Leatherman**[1,3]

[1]School of Biological Sciences, University of Northern Colorado, Greeley, CO

[2]Present address: University of Colorado, Anchutz Medical Campus, Aurora, CO

Abstract

The *Drosophila* testis is a model organism stem cell niche in which two stem cell populations coordinate together to produce sperm; thus, these stem cells must be balanced in the niche. *Merlin,* a tumor-suppressor and human disease gene required for contact inhibition of proliferation, is known to limit the proliferation of the somatic cyst stem cells in the testis niche. *Expanded* encodes a protein that is structurally similar to Merlin in *Drosophila,* and is semi-redundant with *Merlin* in multiple tissues. We found that *expanded* depletion caused similar cyst lineage cell over-proliferation as observed with *Merlin,* and double mutants showed more severe phenotypes than either gene individually. Thus, these genes have partially redundant functions in the cyst lineage cells of this niche. We also expressed non-phosphorylatable constitutively "tumor suppressing" alleles of *Merlin* in cyst lineage cells, and surprisingly, we observed a similar cyst lineage over-proliferation phenotype. Merlin is known to impact multiple different signaling pathways to exert its effect on proliferation. We found that the *Merlin* loss of function phenotype was associated with an increase in MAPK/ERK signaling, consistent with Merlin's established role in transmembrane receptor inhibition. Constitutive *Merlin* displayed a reduction in both MAPK/ERK signaling and PI3K/Tor signaling. PI3K/Tor signaling is required for cyst cell differentiation, and inhibition of this pathway by *Merlin* activation phenocopied the Tor cyst lineage loss of function phenotype. Thus, Merlin impacts and integrates the activity of multiple signaling pathways in the testis niche. The ability of Merlin to dynamically change its activity via phosphorylation in response to local contact cues provides an intriguing mechanism whereby the signaling pathways that control these stem cells might be dynamically regulated in response to the division of a neighboring germ cell.

Keywords

Drosophila; testis; stem cell; niche; *Merlin*; *expanded*

[3]Corresponding author: Judith.leatherman@unco.edu.

Introduction

The *Drosophila* testis is a well-studied model organism stem cell niche that has been instructive to our current understanding of how adult stem cells are maintained by their tissue microenvironment. In this niche, two distinct stem cell populations produce cells that must coordinate together to achieve sperm production throughout the lifetime of male fruit flies. Since the numbers of differentiating progeny from the two stem cell types must be balanced, it has long been thought that mechanisms exist to coordinate the stem cell divisions of these two populations. Although some aspects of their coordination have been described, the details of the process remain largely unresolved.

In the *Drosophila* testis niche, stem cells are defined by their tissue position, in contact with a small clump of nondividing somatic cells called the hub [1]. Germline stem cells (GSCs) divide so that one daughter remains in contact with the hub and self-renews, while the other daughter loses its hub contact and becomes fated to differentiate [2]. The second stem cell population, the cyst stem cells (CySCs), intermingle with the GSCs around the hub, and divide to produce cyst cells which engulf (or “encyst”) differentiating germ cells and guide them through differentiation. Since two cyst cells always encyst each differentiating germ cell, a ratio of two cyst: one germline cell is needed for sperm production. The encysted differentiating germ cell undergoes four transit-amplifying mitotic divisions as spermatogonia, followed by meiosis and spermatocyte differentiation. Cyst cells, by contrast, immediately withdraw from the cell cycle as they differentiate, but they continue to stretch their cytoplasm to engulf the growing cyst of differentiating germ cells, isolating them from their surroundings.

One way that the two stem cell populations achieve their balance of differentiating progeny is by maintaining roughly two CySCs for every GSC in the niche. This balance can be disrupted by changes in CySCs that increase their competitiveness, causing them to displace GSCs from the niche. Both *socs36E* and *madm* depletion increase CySC competitiveness, and they both appear to act through an increase in CySC MAPK/ERK signaling [3–6]. Coordination has also been investigated between individual GSCs and their flanking CySCs. Although the cell cycles of the adjacent stem cells do not seem to be coordinated, the GSCs have a delay in the final step of cytokinesis, abscission. Completion of this final separation between the GSC and its differentiating daughter requires nonautonomous encystment by CySCs/cyst cells via Rac activation through EGFR [7]. Finally, Merlin, a tumor-suppressor protein best known for mediating contact inhibition of growth, has been implicated in CySC proliferation control. Loss of *Merlin* caused accumulation of excess cyst lineage cells in the niche, and this could be partially rescued through an increase in E-cadherin, suggesting that adherens junction-mediated contact inhibition plays a role in detecting and maintaining the overall balance between germline and cyst lineage cells in the niche [8].

Merlin is a multifunctional protein that resides at the cell cortex, acting to sense information from the extracellular environment and integrate it with intracellular responses on signaling pathways, ultimately leading to changes in cell proliferation, fate, shape, migration, and survival [9]. Loss of function mutation of the *neurofibromatosis* 2 (*NF2*) gene, which encodes the Merlin ortholog in mammals, causes tumorigenesis in both humans and mice

[10–12]. In cell culture, *NF2*-deficiency prevents stable adherens junctions from forming between cells, and these cells cannot undergo contact-dependent inhibition of proliferation [13].

Similarly to the closely related proteins of the ERM family (ezrin, radixin, moesin), the activity of Merlin is regulated by phosphorylation near the C-terminus (Ser518 in mammals, Thr616 in *Drosophila*) [14, 15]. Unphosphorylated Merlin is able to self-associate between its N- and C-termini, creating a closed conformation which is also the active tumor suppressor form promoting growth inhibition. Phosphorylated Merlin forms a less closed conformation which inactivates its tumor suppressor activity, allowing proliferation [16, 17]. Merlin is activated by the phosphatases MYPT1-PP1δ in mammals, and flapwing in *Drosophila,* and undergoes inactivating phorphorylation by p21 activated kinase (PAK) and Protein kinase A in mammals, and Slik kinase in *Drosophila* [18–22].

When Merlin is in its unphosphorylated tumor suppressor conformation, it influences a wide array of signaling pathways including EGFR and other transmembrane receptors, Rac1, Hippo, and TOR. Active Merlin inhibits receptor tyrosine kinases and other transmembrane signaling receptors by regulating their endocytosis or sequestering them to prevent their interaction with downstream effectors [15, 23]. Rac1 has been shown to be inhibited by Merlin via several mechanisms; directly via inhibition of membrane association, or indirectly through effects on its activator Pak, or its negative regulator Rich1 [24–26]. Active Merlin affects Hippo signaling via interaction with Kibra at the plasma membrane, leading to the repressive phosphorylation of the proliferation-promoting YAP (Yorkie in *Drosophila*) [27–30]. Finally, Merlin also acts to inhibit the PI3K/Akt-activated mTOR complex 1 (mTORC1) involved in cellular growth, although the mechanism is unclear [31].

In *Drosophila,* a second FERM-domain tumor suppressor protein, expanded, physically interacts with Merlin, colocalizing to the apical adherens junction region of epithelia [32]. While mutations in either gene alone produce over-proliferation defects of the eye and wing discs, double mutants show much more severe overgrowth than is seen with either individual mutant condition, suggesting that they are partially redundant [33]. Merlin and expanded also work together to regulate transmembrane receptor endocytosis, and both are involved in Hippo signaling [15, 27, 29]. A requirement for *expanded* has been described in the differentiating cyst cells of the testis, where it functions to non-autonomously limit proliferation of the encysted transit-amplifying spermatogonia [34].

In this study, we examined whether *expanded* functions along with *Merlin* to regulate the cyst lineage cells of the *Drosophila* testis niche. We also explored the mechanism of Merlin action in the testis, comparing signaling differences in loss and gain of function conditions. Our results suggest that Merlin dynamically regulates multiple signaling pathways in the testis stem cells to coordinate their behavior.

Materials and Methods

Fly lines, crosses, and husbandry

All stocks and crosses were maintained at room temperature. Adult progeny of crosses were transferred to 29° for varying incubation times (4-14 days) to induce Gal4 activity, or to inactivate temperature sensitive alleles. Fly stocks included: c587 Gal4, Tj Gal4, Canton S (wild type), Mer^{ts1}[35] (gift from Yukiko Yamashita), UAS *Mer* RNAi (Trip JF02841)[36], UAS *expanded* RNAi (Trip HMS00875)[36], UAS Mer^{T616A} [19](gift from Richard Fehon), UAS $Mer^{1\text{-}600}$ [37](gift from Richard Fehon), $Egfr^{ts1a}$ [38], *tsc2 (gig)* RNAi (Trip HMS01217) [36], and Vasa GFP [39].

Immunofluorescence

Testes were dissected in Ringers solution, then fixed in 4% formaldehyde in Buffer B (75 mM KCl, 25mM NaCl, 3.3mM $MgCl_2$, 16.7mM KPO_4) plus 0.1% Triton X-100 for 20 minutes. Testes were washed in PBTx (1X PBS, 0.1% triton X-100), blocked (4% normal donkey serum in PBTx), and stained with primary antibodies overnight at 4°C. Primary antibodies used were mouse anti-fasciclin 3 (1:20, DSHB), goat anti-vasa (1:200, Santa Cruz sc-26877), rabbit anti-vasa (1:200, Santa Cruz, sc-30210), guinea pig anti-Tj (1:10,000, gift from Dorothea Godt [40]), rabbit anti-zfh1 (1:5000, gift from Ruth Lehmann [41]), rat anti-Ecadherin (1:20, DSHB), mouse anti-phosphohistone H3 (1:500, AbCam 14955), chicken anti-GFP (1:1000, AbCam 13970), rabbit anti-GFP (Invitrogen A6455) rabbit anti-Phospho-p44/42 MAPK (dpErk) (1:500, Cell Signaling 9101), rabbit anti-phospho4E-BP1 (Cell Signaling 2855) and mouse anti-Eya (1:20, DSHB). Samples were washed in PBTx, then incubated in secondary antibodies for at least 1 hour. All secondary antibodies were from Jackson ImmunoResearch (1:400). Samples were stained with Hoechst 33342 (1 ug/mL), and washed in PBTx. Testes were mounted on slides in 90% glycerol, 1X PBS with 2% N-propyl gallate anti-bleaching agent and stored at −20°.

EdU Labeling

Edu labeling was performed using the Click-iT EdU Cell Proliferation Kit for Imaging, Alex Fluor 647 (Molecular Probes C10340). EdU (5-ethynyl-2-deoxyuridine) is a thymine analog that incorporates into DNA in S-phase. Testes were dissected in Ringers, then incubated in 10 uM EdU in Ringers for 30 minutes. Fix and immunofluorescence stain was performed as described, followed by visualization of EdU with the click-it reaction as per the manufacturer's instructions.

Imaging, quantitation, and statistical analysis

Stained testes were visualized using a Zeiss 700 confocal microscope. Z stacks of each testis were taken at .5μm intervals. Care was taken to image the depth of the entire testis for whole-testis cell counts (usually about 50 slices). ImageJ was used for image analysis. Cell counts were initially performed by identifying cells in a single channel in three dimensional space with the 3D Objects Counter or the Aggregate Detector plugins in ImageJ. Intensity thresholds and minimum volume settings were varied for each stain in order to optimize the identification of individual cells; once optimized, identical settings were used for control and

experimental testes within each experiment. Following 3D object identification, all analyses were manually checked and corrected. For example, if the Aggregate Detector plugin erroneously counted three cells in one group, then two cells were added to the final tally. For statistical analysis with three or more groups, one-way analysis of variance (Anova) was performed followed by Tukey-Kramer post hoc tests. Comparison of two groups was performed by two sample unequal variance Student t-test. Chi square goodness of fit test was used to compare percent of testes with a given phenotype to that observed in controls.

Immunofluorescence against phosphorylated proteins

For dpErk and p4E-BP1 stains, phosphatase inhibitors (180mM KCl, 50mM NaF, 10mM $NaV0_4$ and 10mM β-glycerophosphate in 10mM Tris HCl, pH 6.8) were added to dissection and fixative solutions [3]. To accurately compare dpERK and p4E-BP1 staining intensities, identical antibody staining mixes and staining conditions were used between experimental and stain-matched controls. Identical microscope imaging settings between the stain-matched samples were used. Because phospho-stains can fade with time, the sample hypothesized to have the lower stain intensity was always imaged first to eliminate fading bias. In order to compare dpERK or p4E-BP1 intensity in only the relevant regions of the testes, the 3D objects counter in ImageJ was used to generate a 3D surface map of all Tj+ cyst cell nuclei, then using the masking/ redirect function in ImageJ, average intensity measurements for the region of each Tj cell nucleus were taken based on the dpERK or p4E-BP image. Statistical analysis was performed by Student t-test, using each cell as an individual n value. Alternatively, all intensity values for cells in a single testis were averaged, then the average intensities per testis were used as individual n values in comparisons between control and experimental samples. Either method of analysis gave statistical significance.

Permeability assay

To visualize defects in encystment, a permeability assay adapted from Guy Tanentzapf's protocol was performed [42]. Glass bottom cover dishes were coated with Poly-L-lysine (1.0 mg/mL in 100mM Tris pH 8.5) overnight at 4°C to allow testes to adhere to the glass [43]. Dissected testes were transferred to the glass bottom dish and allowed to adhere. 10 kDa Dextran conjugated to Alexa fluorophore-647 (Invitrogen D22914) at a final concentration of 0.2 μg/μl in Schneider's *Drosophila* Medium (Gibco 21720-024) was added to the sample and allowed to incubate for 30 minutes prior to imaging. Samples were then imaged as described above and analyzed in ImageJ.

Results

Merlin and *expanded* depletion cause an increase in cyst lineage cells and a decrease in GSCs

Previously it was reported that Merlin accumulates at the cell cortex of cyst lineage cells in the *Drosophila* testis [8]. Expanded has also been reported to accumulate in the testis, and a lacZ enhancer trap line showed reporter accumulation in the cyst lineage cells near the hub, overlapping with the CySC marker Zfh1 [44, 45]. We depleted *Merlin* using a temperature sensitive loss of function allele (Mer^{ts1}), and we depleted *expanded* via cyst lineage

expression of an RNAi transgene [35, 36]. After aging flies at 29°C for seven days to both inactivate the *Mer*^{ts} allele and activate Gal4-driven expression of the transgenic shRNA against *expanded*, we stained and imaged testes, and counted stained cells through all Z sections of the 3D imaged testes. As previously reported, we found that Merlin inhibition by incubation of *Mer*^{ts} at the nonpermissive temperature caused accumulation of excess cyst lineage cells marked by Traffic Jam (Tj) expression, compared to control testes (Figure 1A, B, quantitation in 1H)[8, 46]. Ablation of *expanded* by RNAi, or *Merlin* and *expanded* together also caused accumulation of excess Tj-positive cyst lineage cells compared to controls (Figure 1C, D). Interestingly, the number of Tj-positive cells was highest in the *expanded*-only condition (Figure 1H); this observation will be further discussed below.

We also counted the number of GSCs in the *Merlin* and *expanded* single and double mutant conditions, identifying GSCs as vasa-positive germ cells that touch the hub. Control testes had an average of 8.4 GSCs per testis (Figure 1A, quantitation in 1I). We found a slight but statistically significant reduction in the number of GSCs with either *Merlin* or *expanded* ablation, down to 5.9 and 6.7 GSCs per testis respectively (Figure 1B, C, quantitation in 1I). In double mutant testes the number of GSCs dropped even further, to 2.9 per testis on average (Figure 1D, I). Rarely, we even observed testes in which all GSCs were lost (2 out of 22 testes, Figure 1G). Thus, inhibition of both genes led to a more severe GSC loss phenotype, suggesting some functional redundancy of *Merlin* and *expanded* with regard to their nonautonomous influence on GSC number. The gain in cyst lineage cells at the expense of GSCs indicates that *Merlin* and *expanded* mutant cyst lineage cells occupy the niche more effectively than usual, outcompeting GSCs for a spot next to the hub.

In this tissue, while germline cells undergo a period of transit-amplifying mitotic division as they differentiate, CySCs are the only cyst lineage cells that normally divide. Therefore, cycling cyst lineage cells are restricted to the region immediately adjacent to the hub (within two germ cell diameters of the hub, or about 15 microns, Figure 1A, A', arrows). We marked cells in S phase by labeling with the thymidine analog EdU (5-ethynyl-2'-deoxyuridine), followed by visualization with the Click-iT reaction (ThermoFisher). We examined testes with *Merlin* or *expanded* depletion and noticed rare EdU-positive, Tj-positive cells at a further distance from the hub than usual (Figure 1A–D, arrows, A'-D' show EdU and Fas3 hub stain only). While control testes with EdU+ cyst cells outside the niche area were extremely rare (4.5% of testes), we found that *Merlin, expanded,* and double mutant testes had 56%, 43%, and 78% of testes, respectively, with at least one EdU+ cyst cell further than two germ cell diameters from the hub (Figure 1J). We also labeled mitotic cells by phosphohistone H3 (pH3) stain. In control testes, mitotic Tj-positive cyst lineage cells were restricted to the niche area (Figure 1E, E', arrow), and we observed a negligible fraction of testes with mitotic cyst cells further than two germ cell diameters from the hub in control, *Merlin,* or *expanded* single mutants (Figure 1K). However, 21% of double mutant testes showed at least one pH3-positive cyst cell away from the hub (Figure 1F, F', arrow, quantitation in 1K). Thus, *Merlin* and *expanded* depletion caused cyst cells to cycle away from the hub, and the two genes were partially redundant with regard to effects on this phenotype. The observed higher frequency of cells in S phase versus mitosis is expected, since S phase is much longer in duration than mitosis. We speculate that these rare cycling cells outside the niche are the extra cyst cells produced from the *Merlin/expanded*-induced

deregulation of contact inhibition, which do not have sufficient differentiating germ cells available to encyst; these non-encysting cells have also been previously described as “lone” cyst cells [8].

Interestingly, the number of Tj-positive cells was significantly higher in the *expanded*-alone ablation than the *Merlin*-alone or the double mutant testes (Figure 1H). We speculated that this may partially be due to the previously reported requirement for *expanded* to promote differentiation of late cyst cells and their encysted spermatogonia into spermatocyte differentiation (Sun et al. (2008) showed that ablation of *expanded* in cyst cells led occasional spermatogonial cysts to continue past the normal four transit-amplifying mitotic divisions) [34]. If spermatogonial cysts persisted past the normal 16-cell cysts with *expanded* depletion, more overall Tj+ cells would be expected, since the Tj marker turns off soon after the transition into spermatocyte differentiation. Although we observed occasional spermatogonial cysts larger than 16 cells in *expanded* RNAi testes, in agreement with the previous report (data not shown)[34], these few rare cysts seemed insufficient to explain the difference of approximately 30 Tj+ cells between testes with *Merlin* and *expanded* ablation (Figure 1H).

We noted several other points regarding the increased number of Tj+ cyst cells. First, since the double mutants did not have as many excess Tj+ cells as *expanded* alone, it is clear that the *expanded* phenotype was partially suppressed by *Merlin* mutation. We also observed that most testes with *Merlin* mutation appeared thin compared to controls or testes with *expanded* inhibition, with fewer than normal cysts of transit-amplifying spermatogonia (Figure 1B, D). We quantified this observation by counting the cyst cells that encyst these late-stage spermatogonia, which normally stain for both Tj and high levels of the late cyst cell differentiation marker Eyes absent (Eya) [47]. While control testes and *expanded* knockdown had similar numbers of dual-positive Tj+ Eya+ cells (22.5 and 25.7 per testis, respectively), *Merlin* mutant or double mutant testes had significantly fewer of these cells (4.9 and 7.8 per testis, respectively, Supplemental Figure 1). This difference reveals divergence in the functions of Merlin and expanded in late cyst cells. While inhibition of either gene led to excess cyst lineage cells in the vicinity of the niche, only *Merlin* inhibition caused loss of late-stage cyst cells, along with concomitant loss of the transit-amplifying spermatogonial cells they encyst. Loss of late spermatogonial cysts due to premature differentiation into spermatocytes has previously been observed from hyperactivation of cyst cell EGFR signaling [48]; thus one of Merlin’s normal functions may be to inhibit EGFR signaling in differentiating cyst cells (investigated further below).

Constitutively active Merlin causes similar phenotypes as loss of function Merlin

The activity of Merlin is regulated by phosphorylation. The unphosphorylated form of Merlin is active as a tumor suppressor. Activating dephosphorylation occurs in response to a cell achieving contact with its neighbors, and in this form Merlin inhibits proliferation via its effects on multiple signaling pathways [9]. Phosphorylation at Thr616 inactivates Merlin’s tumor suppressor functions, producing an inactivated state similar to a loss of function gene mutation; Merlin becomes inactivated by phosphorylation when cells are not contact inhibited, thereby allowing normal cell signaling and proliferation to proceed [19]. Since the

regulation of expanded by phosphorylation is not as well understood, we decided to focus our remaining investigations on *Merlin* only.

To further investigate the function of *Merlin* in testes, we used the Gal4 UAS system to express two different transgenic "constitutive" alleles of *Merlin* in the cyst lineage: a non-phosphorylatable transgene, Mer^{T616A}, or a truncated transgene, $Mer^{1\text{-}600}$, in which the regulatory C-terminus of the protein is deleted [19, 37]. Surprisingly, we observed some of the same phenotypes as the loss of function experiments. The number of Tj+ cyst lineage cells per testis increased; control testes had an average of 59 Tj+ cells, while an average of 74 and 79 Tj+ cells were observed in testes expressing the Mer^{T616A} or $Mer^{1\text{-}600}$ constitutive alleles respectively (Figure 2A–C, quantitation in 2D). We also observed a decrease in the number of GSCs from 6.7 in control testes to 3.6 and 5.6 on average with the Mer^{T616A} and $Mer^{1\text{-}600}$ constitutive alleles, respectively (Figure 2E). We labeled cells in S phase with EdU, and found that while control testes had no Tj+ EdU+ cells away from the hub, both constitutive *Merlin* alleles produced testes with Tj+ EdU+ cyst cells away from the hub (23% and 25% of testes for Mer^{T616A} and $Mer^{1\text{-}600}$ respectively, quantitation in Figure 2F, testis images shown in Supplemental Figure 2).

Despite the similarities in phenotype between the loss and gain of function experiments, there were also differences. Zfh1 is a marker for CySCs and their immediate daughters, and therefore its expression is normally restricted to cyst lineage cells very close to the hub [45]. We found that testes with constitutive *Merlin* accumulated more Zfh1+ cells than controls (average of 25.7 per testis for $Mer^{1\text{-}600}$ versus 19.3 for controls), and these cells were often at a further than usual distance from the hub, a phenotype not observed in *Merlin* mutants (Figure 3A, A', B, B', quantified in 3C)[8]. The increase in Zfh1+ cells with constitutive *Merlin* was accompanied by a decrease in Eya-staining differentiating cyst cells, and these cells were found at a further distance away from the hub than in control testes (Figure 3A",B", arrows, quantified in 3D). In some testes, we observed clumps of spermatogonia that were greater than 16-cells (Figure 3E, arrows). We also occasionally observed an over-proliferation phenotype in which the entire testis filled with Zfh1-positive cells intermingled with GSC-like spermatogonia (Figure 3F). This phenotype most likely arose as a secondary result of the misexpression of Zfh1 in cyst cells away from the hub [45]. Finally, we investigated whether the differentiating cyst cells with constitutive *Merlin* properly encysted the differentiating germline cells by testing whether the permeability barrier was functional. We soaked testes in 10kDa fluorescent dextran dye as previously described [49], and found that dye was not able to permeate between individual germ cells within a differentiating cyst in control or *Merlin*-depleted testes, but was able to permeate in some of the cysts with expression of either *Merlin* constitutive allele (Supplemental Figure 3). Thus, constitutive *Merlin* expression may have led to failure in the establishment or maintenance of the cyst cell permeability barrier. We cannot rule out the possibility, however, that the cells with dye permeation are excess accumulated early-stage zfh1+ cells and spermatogonia, which would not yet be expected to have a permeability barrier.

Merlin regulates dpERK accumulation in cyst lineage nuclei

Since the *Merlin/expanded* loss of function, and the *Merlin* gain of function testes confusingly had partially similar phenotypes, we decided to further investigate the reasons for the observed phenotypes. When Merlin is in its active unphosphorylated state due to contact inhibition inputs, it responds by impacting multiple signaling pathways, integrating signals that inhibit proliferation. In *Drosophila, Merlin* and *expanded* have been most extensively studied in their role in Hippo signaling, where they function together with Kibra at the apical cortex to activate Hippo signaling, thereby leading to Yorkie inactivation and mitotic quiescence [28, 29]. However, the *Merlin* testis phenotype appears to not involve the Hippo pathway, as neither constitutive *yorkie* or *hippo* knockdown were able to phenocopy the *Merlin* mutant testis phenotype [8].

Another well-established function of Merlin is to inhibit transmembrane signaling receptors [15]. We hypothesized that loss of *Merlin* could be leading to increased somatic MAPK/ERK signaling from derepression of EGFR [3]. We inactivated Merlin by incubation of Mer^{ts} males at the nonpermissive temperature, then stained testes with diphosphoERK (dpERK) antibody. As previously reported, dpERK accumulated in cyst lineage cells, both in nuclei, colocalized with the nuclear Tj stain, and in the cytoplasmic projections of cyst cells that wrapped around clusters of germ cells (Figure 4A, A”). Mer^{ts} testes accumulated more Tj+ cells than controls, as we showed above, and these cells appeared to accumulate higher levels of dpERK than control testes, both in nuclei and cytoplasmic projections around cysts of germ cells (Figure 4A, A”, B, B”). In order to quantify this result, we used the 3D Objects Counter in Image J to generate a 3D surface map of all Tj+ nuclei, and this map was used to limit the measurements of dpERK intensity to only include cyst lineage cell nuclei (Figure 4A’ and B’ show Tj stain, A”’ and B”’ show the dpERK accumulation limited to Tj stained nuclei). See methods for additional details and precautions taken to ensure intensity measurements were comparable between stain-matched samples. We found a statistically significant increase in dpERK staining intensity in Mer^{ts} cyst cell nuclei compared to stain-matched controls (Figure 4C). Therefore, one function of Merlin in normal testes is to dampen MAPK/ERK signaling through EGFR inhibition (and possibly through inhibition of other transmembrane receptors).

Based on previous reports in the literature on cell competition in the niche, the increase in ERK signaling is the likely reason that *Merlin* mutant CySCs can nonautonomously decrease the number of GSCs, outcompeting them in the niche [3]. Increased ERK signaling in cyst cells from EGFR overactivation has also been shown to cause encysted spermatogonia to bypass their transit-amplifying mitotic divisions [48]. Thus, increased dpERK accumulation can also explain the thinner appearance of the Mer^{ts} testes with fewer spermatogonial germ cell cysts, and the decrease we observed in the number of differentiating cyst cells that are both Tj and Eya-positive (Supplementary Figure 1).

We also examined dpERK accumulation when constitutive *Merlin* alleles were expressed, and again compared staining intensity within the cyst cell nuclei using a Tj 3D surface map (Figure 5 A’, A”’, B’, B”’). We found that expression of either Mer^{T616A} or $Mer^{1\text{-}600}$ promoted a statistically significant reduction in dpERK staining intensity compared to stain-matched controls (Figure 5A”, B”, C, D). Thus, when Merlin is in its active tumor

suppressor state, it inhibits ERK signaling in the testis cyst lineage cells. Based on previous reports in the literature, we think this signaling change is responsible for some of the phenotypes we observed with constitutive *Merlin*. Reduced dpERK signaling has been shown to cause spermatogonial proliferation [50, 51], a phenotype we occasionally observed with constitutive *Merlin* (Figure 3E). EGFR signaling in the testis activates Rac1, which is required for encystment [52]; thus, the encystment failure we observed with constitutive *Merlin* (Supplemental Figure 3) may have resulted from activated Merlin's inhibition of EGFR signaling or Merlin's direct regulation of Rac1 [24, 25].

Constitutive Merlin represses PI3K/Tor signaling

Many of the phenotypes we observed with constitutive *Merlin* remained puzzling to us, as they did not seem attributable to a reduction in EGFR or ERK signaling. Human NF2 patients develop *nf2/Merlin* loss of function tumors that over-activate TOR signaling, and this signaling increase is attenuated when wild type Merlin is reintroduced, indicating that one function of Merlin is to inhibit Tor signaling [31, 53]. In the *Drosophila* testis, activation of PI3K/Tor signaling occurs in the immediate daughters of CySCs, and is critical for their differentiation [54]. Somatic depletion of Akt or Tor resulted in accumulation of Zfh1-positive cyst lineage cells far from the hub, a reduction in the expression of the differentiation marker Eya, and erroneous entry of cyst cells into S phase away from the hub [54]. The phenotype reported for loss of Tor signaling was strikingly similar to what we observed with constitutive *Merlin* expression.

To test whether constitutive Merlin repressed Tor signaling, we used an antibody against a direct target of Tor phosphorylation, phospho4E-BP1, an eIF4 binding protein [55]. Previously this Tor signaling reporter was shown to accumulate at high levels in immediate daughters of CySCs, approximately two germ cell diameters from the hub [54]. In our hands, phospho4E-BP1 accumulated in the cytoplasm and nucleus of differentiating cyst cells, a slightly broader domain than previously reported (Figure 6A–A"). Testes with Mer^{T616A} expression showed strong reduction in phospho4E-BP1 staining intensity compared to stain-matched controls (Figure 6B–B"). In order to quantify this result, we again used the 3D Objects Counter in Image J to generate a 3D surface map of all Tj+ nuclei, and this map was used to limit the measurements of p4E-BP1 intensity to only include cyst lineage cell nuclei. We found a statistically significant decrease in p4E-BP1 staining intensity in Mer^{T616A} cyst cell nuclei compared to stain-matched controls (Figure 6C). As the brightest regions of p4E-BP1 stain in control testes were cytoplasmic (compare Figure 6A' and A"), this quantitation is likely an underestimate of the actual difference. Thus, constitutive *Merlin* leads to repression of Tor signaling in the testis. Multiple aspects of the constitutive *Merlin* phenotype we observed—accumulation of excess Zfh1-positive cells, a reduction in Eya-positive cells, and division of cyst cells away from the hub—are likely the result of decreased Tor signaling in the cyst lineage [54].

EGFR and Tor signaling changes rescue aspects of the Merlin loss and gain of function phenotypes

If the *Merlin* loss of function phenotype resulted primarily from an increase in EGFR/MAPK signaling, the phenotype should be able to be rescued by dampening EGFR

signaling. In *Mer^{ts}* testes, we reduced EGFR signaling by inclusion of one copy of the *Egfr^{ts1a}* temperature sensitive mutant allele [38]. As previously observed, *Mer^{ts}* testes showed an increase in Tj+ cells, a decrease in GSCs, and cyst cells cycling away from the hub, compared to testes from either control or *Egfr^{ts1a}* heterozygotes (Figure 7A, B, quantitation in 7F–H). Inclusion of one *Egfr^{ts1a}* allele in the *Mer^{ts}* flies reduced the number of Tj+ cells back to control levels (Figure 7C, F). However, inclusion of one *Egfr^{ts1a}* allele was not able to rescue other aspects of the *Mer^{ts}* phenotype, including GSC number and cycling of cyst cells away from the hub (Figure 7G, H). Thus, EGFR heterozygosity rescued some, but not all aspects of the *Mer* mutant phenotype. Failure of *EGFR* heteozygosity to rescue some phenotypes could mean that another pathway regulates these aspects of the *Merlin* phenotype, or it could be that EGFR *does* regulate these phenotypes, but the protein levels are not limiting with regard to their requirement for these functions.

We also tried to rescue the constitutive *Merlin* phenotype by boosting Tor pathway signaling. Normally, PI3K/Akt signaling leads to repression of TSC 1 and 2, thereby allowing Rheb to activate Tor. To boost PI3K/Akt signaling, we knocked down TSC2 by expression of an RNAi transgene. As we previously showed, expression of the *Mer^{T616A}* allele led to an increase in the number of Tj+ cells per testis compared to controls (Figure 7D, I). Inclusion of TSC2 RNAi restored Tj+ cell numbers back to control levels, indicating that at least some aspects of the constitutive *Mer* phenotype could be rescued by increasing Tor signaling (Figure 7E, I). Thus, both EGFR/MAPK and PI3K/Tor signaling pathways are impacted by Merlin in the cyst lineage cells and contribute to the phenotypes we observed. Given Merlin's ability to affect a wide array of transmembrane signaling receptors, we cannot rule out the possibility that additional pathways might be impacted by Merlin.

Model for Merlin as a dynamic signaling regulator in the testis niche

Merlin is known to act as a tumor suppressor when it is activated by contact inhibition, inhibiting cell division via attenuation of various signaling pathways. Although we do not fully understand how contact inhibition regulates Merlin in the *In vivo* testis (see discussion), we do know the normal outcome that only CySCs divide. Furthermore, they divide when more cyst cells are needed, somehow coordinating with the neighboring GSCs to produce the proper number of cells to encyst available germ cells. Our data is consistent with a model in which the activity of Merlin is dynamic in CySCs (Figure 8). When new cells are needed, Merlin becomes inactivated, mitosis can proceed, and this is accompanied by increases in EGFR and Tor signaling. When new cyst cells are not needed, contact inhibition (possibly with other cyst lineage cells) activates Merlin, and mitosis and signaling pathways including EGFR and Tor are inhibited. As differentiating cyst cells engulf differentiating germ cells, Merlin becomes activated here as well, inhibiting mitosis and attenuating EGFR and Tor signaling, thereby allowing the appropriate number of transit-amplifying divisions to occur [48]. Although expanded clearly has some redundant functions with Merlin, we did not investigate how it regulates signaling in the testis and thus we did not include expanded in our model.

This model would provide a mechanism by which individual CySCs could respond to their neighboring cells, dividing only when needed through modulation of Merlin activity. This

idea of dynamic regulation of signaling within CySCs contrasts with the prevailing view that signaling in cell populations in the niche is steady state (for example, that all CySCs are always undergoing identical signaling). Further confirmation of dynamic signaling awaits live imaging using sensors for Merlin activity or signaling pathway activation.

Discussion

In this study, we show that *Merlin* and *expanded* have partially redundant functions in the cyst lineage cells of the testis. Single or double mutant conditions led to similar phenotypes, with an increase in the overall number of cyst lineage cells, a reduction in GSCs, and improper entry into S phase outside of the niche. One well-documented function of Merlin and expanded is to repress signaling through transmembrane receptors including EGFR, and consistent with this, we observed an increase in dpERK accumulation in cyst lineage nuclei when *Merlin* was inhibited [15]. The *Merlin* and *expanded* mutant phenotypes likely arise primarily from this defect [3, 48, 52]. Although the GSC reduction phenotype was not able to be rescued by the genetic interaction experiment of introducing *Egfr* heterozygosity, we think this result is inconclusive as the receptor may not be a limiting factor in this phenotype. We did try to further reduce EGFR signaling by expression of a dominant negative transgene (data not shown), but the *Merlin + Egfr*-depleted testes were dominated by the severe phenotype that has previously been reported for *Egfr* loss of function, making quantitative comparisons of cell numbers difficult [48, 50, 51].

The one phenotype we observed that is not consistent with previous reports of ERK signaling increase is the entry of cyst cells into S phase away from the hub. We think the cyst cells that continue dividing are likely excess cells that did not find a germ cell to encyst. These cells did not continue dividing indefinitely, however; most were found within the spermatogonial region of the testis, and large tumors of cells were never observed. It could be that their erroneous division was slow, they died, or their division remained dependent upon locally available growth factors from the hub. The lack of cell cycle withdrawal of cyst cells in the absence of germ cells in consistent with reports in the literature in which cyst cells proliferate in the absence of the germline [56].

By contrast, expression of activated *Merlin* alleles, always in tumor suppressor form, led to a decrease in both ERK and PI3K/Tor signaling, and the phenotypes we observed are likely due to both of these signaling changes. The presence of cysts of spermatogonia with more than 16 cells, and failure of encystment are predictable results of EGFR inhibition [50–52]. The increased numbers of Zfh1+ cells that accumulated outside the niche, reduction in Eya+ differentiating cyst cells, and improper entry of cyst cells into S phase outside of the niche are likely all the result of inhibition of Tor signaling, and prevention of the Tor-mediated differentiation program [54]. To our knowledge, this study is the first report of Merlin regulating Tor signaling in *Drosophila.*

The one phenotype we observed with constitutive Merlin that we do not understand fully is the decrease in the number of GSCs. This phenotype has been most closely linked to GSCs being outcompeted in the niche from *elevated* ERK signaling [3]. In this situation of reduced

ERK signaling, we speculate the phenotype may occur from the overabundance of Zfh+ cells that accumulate in the niche region due to Tor signaling reduction.

The model we proposed in Figure 8 suggests that Merlin activity is dynamic in CySCs, changing in response to local contact inhibition cues. Contact inhibition is easy to understand in a cell culture context—once cells start to touch each other, Merlin becomes activated by dephosphorylation. In an *in vivo* tissue setting, contact inhibition is harder to understand, as cells always touch other cells. There is growing evidence that cyst lineage cells are polarized, and this polarization is critical for their function [57–60]. Contact inhibition must occur at a particular location in a polarized cell—via cadherins at adherens junctions. E-cadherin accumulates most strongly at two locations in cyst lineage cells—between CySCs and the hub, and between cyst cell "partners" that cooperate to encyst a germ cell [8]. We speculate that Merlin activity in CySCs is regulated specifically by contact with its CySC partner cell. When new cyst cells are not needed, the partner CySCs touch on the distal side of the GSC from the hub, contact inhibition is achieved, and Merlin is activated, inhibiting mitosis. New CySCs are needed when the neighboring GSC has just divided; GSCs have a delayed abscission with their daughter cell, and during this time the CySC might loss contact with its partner CySC, thereby inactivating Merlin and allowing mitosis to proceed. Interestingly, activation of EGFR and Rac in CySCs is known to be required for GSC abscission, consistent with a need to inactivate Merlin [7].

Although *Merlin/NF2* is a human disease gene with significant clinical relevance, its pleiotropic effects on cell signaling have obscured a clear understanding of how it functions in a normal *In vivo* setting. Our examination of the effects of Merlin activity in a normal stem cell niche have revealed that a simplistic understanding of its activity as a tumor suppressor is insufficient, but its effects can be understood by investigation of the specific signaling changes that take place, and how those changes uniquely affect the stem cell population under investigation.

Supplementary Material

Refer to Web version on PubMed Central for supplementary material.

Acknowledgements

We thank Yukiko Yamashita, Erika Matunis, Richard Fehon, and the Bloomington *Drosophila* Stock Center for fly stocks. We thank Ruth Lehmann, Dorothea Godt, and the Developmental Studies Hybridoma Bank for antibodies. We thank Steve DiNardo for comments on the manuscript. This work was supported by NIH R15 GM102828 to J.L.

References Cited

1. Hardy RW, et al., The germinal proliferation center In the testis of Drosophila melanogaster. J Ultrastruct Res, 1979. 69(2): p. 180–90. [PubMed: 114676]
2. Yamashita YM, Jones DL, and Fuller MT, Orientation of asymmetric stem cell division by the APC tumor suppressor and centrosome. Science, 2003. 301(5639): p. 1547–50. [PubMed: 12970569]
3. Amoyel M, et al., Socs36E Controls Niche Competition by Repressing MAPK Signaling in the Drosophila Testis. PLoS Genet, 2016. 12(1): p. e1005815. [PubMed: 26807580]

4. Issigonis M, et al., JAK-STAT signal inhibition regulates competition in the Drosophila testis stem cell niche. Science, 2009. 326(5949): p. 153–6. [PubMed: 19797664]
5. Singh SR, et al., Competitiveness for the niche and mutual dependence of the germline and somatic stem cells in the Drosophila testis are regulated by the JAK/STAT signaling. J Cell Physiol, 2010. 223(2): p. 500–10. [PubMed: 20143337]
6. Singh SR, et al., The novel tumour suppressor Madm regulates stem cell competition in the Drosophila testis. Nat Commun, 2016. 7: p. 10473. [PubMed: 26792023]
7. Lenhart KF and DiNardo S, Somatic cell encystment promotes abscission in germline stem cells following a regulated block in cytokinesis. Dev Cell, 2015. 34(2): p. 192–205. [PubMed: 26143993]
8. Inaba M, et al., Merlin is required for coordinating proliferation of two stem cell lineages in the Drosophila testis. Sci Rep, 2017. 7(1): p. 2502. [PubMed: 28566755]
9. Stamenkovic I and Yu Q, Merlin, a “magic” linker between extracellular cues and intracellular signaling pathways that regulate cell motility, proliferation, and survival. Curr Protein Pept Sci, 2010. 11(6): p. 471–84. [PubMed: 20491622]
10. Rouleau GA, et al., Alteration in a new gene encoding a putative membrane-organizing protein causes neuro-fibromatosis type 2. Nature, 1993. 363(6429): p. 515–21. [PubMed: 8379998]
11. Trofatter JA, et al., A novel moesin-, ezrin-, radixin-like gene is a candidate for the neurofibromatosis 2 tumor suppressor. Cell, 1993. 75(4): p. 826. [PubMed: 8242753]
12. McClatchey AI, et al., Mice heterozygous for a mutation at the Nf2 tumor suppressor locus develop a range of highly metastatic tumors. Genes Dev, 1998. 12(8): p. 1121–33. [PubMed: 9553042]
13. Lallemand D, et al., NF2 deficiency promotes tumorigenesis and metastasis by destabilizing adherens junctions. Genes Dev, 2003. 17(9): p. 1090–100. [PubMed: 12695331]
14. Surace EI, Haipek CA, and Gutmann DH, Effect of merlin phosphorylation on neurofibromatosis 2 (NF2) gene function. Oncogene, 2004. 23(2): p. 580–7. [PubMed: 14724586]
15. Maitra S, et al., The tumor suppressors Merlin and Expanded function cooperatively to modulate receptor endocytosis and signaling. Curr Biol, 2006. 16(7): p. 702–9. [PubMed: 16581517]
16. Petrilli AM and Fernandez-Valle C, Role of Merlin/NF2 inactivation in tumor biology. Oncogene, 2016. 35(5): p. 537–48. [PubMed: 25893302]
17. Sherman L, et al., Interdomain binding mediates tumor growth suppression by the NF2 gene product. Oncogene, 1997. 15(20): p. 2505–9. [PubMed: 9395247]
18. Alfthan K, et al., Cyclic AMP-dependent protein kinase phosphorylates merlin at serine 518 independently of p21-activated kinase and promotes merlin-ezrin heterodimerization. J Biol Chem, 2004. 279(18): p. 18559–66. [PubMed: 14981079]
19. Hughes SC and Fehon RG, Phosphorylation and activity of the tumor suppressor Merlin and the ERM protein Moesin are coordinately regulated by the Slik kinase. J Cell Biol, 2006. 175(2): p. 305–13. [PubMed: 17060498]
20. Yang Y, et al., The PP1 phosphatase flapwing regulates the activity of Merlin and Moesin in Drosophila. Dev Biol, 2012. 361(2): p. 412–26. [PubMed: 22133918]
21. Jin H, et al., Tumorigenic transformation by CPI-17 through inhibition of a merlin phosphatase. Nature, 2006. 442(7102): p. 576–9. [PubMed: 16885985]
22. Thaxton C, et al., Neuregulin and laminin stimulate phosphorylation of the NF2 tumor suppressor in Schwann cells by distinct protein kinase A and p21-activated kinase-dependent pathways. Oncogene, 2008. 27(19): p. 2705–15. [PubMed: 17998937]
23. Lallemand D, et al., Merlin regulates transmembrane receptor accumulation and signaling at the plasma membrane in primary mouse Schwann cells and in human schwannomas. Oncogene, 2009. 28(6): p. 854–65. [PubMed: 19029950]
24. Shaw RJ, et al., The Nf2 Tumor Suppressor, Merlin, Functions in Rac-Dependent Signaling. Developmental Cell, 2001. 1(1): p. 63–72. [PubMed: 11703924]
25. Okada T, Lopez-Lago M, and Giancotti FG, Merlin/NF-2 mediates contact inhibition of growth by suppressing recruitment of Rac to the plasma membrane. J Cell Biol, 2005. 171(2): p. 361–71. [PubMed: 16247032]

26. Yi C, et al., A tight junction-associated Merlin-angiomotin complex mediates Merlin's regulation of mitogenic signaling and tumor suppressive functions. Cancer Cell, 2011. 19(4): p. 527–40. [PubMed: 21481793]
27. Hamaratoglu F, et al., The tumour-suppressor genes NF2/Merlin and Expanded act through Hippo signalling to regulate cell proliferation and apoptosis. Nature Cell Biology, 2006. 8(1): p. 27–36. [PubMed: 16341207]
28. Yu J, et al., Kibra Functions as a Tumor Suppressor Protein that Regulates Hippo Signaling in Conjunction with Merlin and Expanded. Developmental Cell, 2010. 18(2): p. 288–299. [PubMed: 20159598]
29. Su T, et al., Kibra and Merlin Activate the Hippo Pathway Spatially Distinct from and Independent of Expanded. Developmental Cell, 2017. 40(5): p. 478–490.e3. [PubMed: 28292426]
30. Zhang N, et al., The Merlin/NF2 Tumor Suppressor Functions through the YAP Oncoprotein to Regulate Tissue Homeostasis in Mammals. Developmental Cell, 2010. 19(1): p. 27–38. [PubMed: 20643348]
31. James MF, et al., NF2/Merlin Is a Novel Negative Regulator of mTOR Complex 1, and Activation of mTORC1 Is Associated with Meningioma and Schwannoma Growth. Molecular and Cellular Biology, 2009. 29(15): p. 4250. [PubMed: 19451225]
32. Boedigheimer MJ, Nguyen KP, and Bryant PJ, Expanded functions in the apical cell domain to regulate the growth rate of imaginal discs. Developmental Genetics, 1997. 20(2): p. 103–110. [PubMed: 9144921]
33. McCartney BM, et al., The neurofibromatosis-2 homologue, Merlin, and the tumor suppressor expanded function together in Drosophila to regulate cell proliferation and differentiation. Development, 2000. 127(6): p. 1315. [PubMed: 10683183]
34. Sun S, Zhao S, and Wang Z, Genes of Hippo signaling network act unconventionally in the control of germline proliferation in Drosophila. Developmental Dynamics, 2008. 237(1): p. 270–275. [PubMed: 18095349]
35. MacDougall N, et al., Merlin, the Drosophila homologue of neurofibromatosis-2, is specifically required in posterior follicle cells for axis formation in the oocyte. Development, 2001. 128(5): p. 665–73. [PubMed: 11171392]
36. Perkins LA, et al., The Transgenic RNAi Project at Harvard Medical School: Resources and Validation. Genetics, 2015. 201(3): p. 843–52. [PubMed: 26320097]
37. LaJeunesse DR, McCartney BM, and Fehon RG, Structural Analysis of Drosophila Merlin Reveals Functional Domains Important for Growth Control and Subcellular Localization. Journal of Cell Biology, 1998. 141(7): p. 1589–1599.
38. Rodrigues AB, Werner E, and Moses K, Genetic and biochemical analysis of the role of Egfr in the morphogenetic furrow of the developing Drosophila eye. Development, 2005. 132(21): p. 4697–707. [PubMed: 16207755]
39. Bence M, et al., Combining the auxin-inducible degradation system with CRISPR/Cas9-based genome editing for the conditional depletion of endogenous Drosophila melanogaster proteins. FEBS J, 2017. 284(7): p. 1056–1069. [PubMed: 28207183]
40. Li MA, et al., The large Maf factor Traffic Jam controls gonad morphogenesis in Drosophila. Nature Cell Biology, 2003. 5: p. 994. [PubMed: 14578908]
41. Broihier HT, et al., zfh-1 is required for germ cell migration and gonadal mesoderm development in Drosophila. Development, 1998. 125(4): p. 655–66. [PubMed: 9435286]
42. Fairchild MJ, Smendziuk CM, and Tanentzapf G, A somatic permeability barrier around the germline is essential for Drosophila spermatogenesis. Development, 2014: p. dev-114967.
43. Lenhart KF and DiNardo S, Somatic cell encystment promotes abscission in germline stem cells following a regulated block in cytokinesis. Developmental cell, 2015. 34(2): p. 192–205. [PubMed: 26143993]
44. Amoyel M, Simons BD, and Bach EA, Neutral competition of stem cells is skewed by proliferative changes downstream of Hh and Hpo. EMBO J, 2014. 33(20): p. 2295–313. [PubMed: 25092766]
45. Leatherman JL and Dinardo S, Zfh-1 controls somatic stem cell self-renewal in the Drosophila testis and nonautonomously influences germline stem cell self-renewal. Cell Stem Cell, 2008. 3(1): p. 44–54. [PubMed: 18593558]

46. Li MA, et al., The large Maf factor Traffic Jam controls gonad morphogenesis in Drosophila. Nat Cell Biol, 2003. 5(11): p. 994–1000. [PubMed: 14578908]
47. Fabrizio JJ, Boyle M, and DiNardo S, A somatic role for eyes absent (eya) and sine oculis (so) in Drosophila spermatocyte development. Dev Biol, 2003. 258(1): p. 117–28. [PubMed: 12781687]
48. Hudson AG, et al., A temporal signature of epidermal growth factor signaling regulates the differentiation of germline cells in testes of Drosophila melanogaster. PLoS One, 2013. 8(8): p. e70678. [PubMed: 23940622]
49. Fairchild MJ, Smendziuk CM, and Tanentzapf G, A somatic permeability barrier around the germline is essential for Drosophila spermatogenesis. Development, 2015. 142(2): p. 268–81. [PubMed: 25503408]
50. Tran J, Brenner TJ, and DiNardo S, Somatic control over the germline stem cell lineage during Drosophila spermatogenesis. Nature, 2000. 407(6805): p. 754–7. [PubMed: 11048723]
51. Kiger AA, White-Cooper H, and Fuller MT, Somatic support cells restrict germline stem cell self-renewal and promote differentiation. Nature, 2000. 407(6805): p. 750–4. [PubMed: 11048722]
52. Sarkar A, et al., Antagonistic Roles of Rac and Rho in Organizing the Germ Cell Microenvironment. Curr Biol, 2007.
53. Giovannini M, et al., mTORC1 inhibition delays growth of neurofibromatosis type 2 schwannoma. Neuro Oncol, 2014. 16(4): p. 493–504. [PubMed: 24414536]
54. Amoyel M, et al., Somatic stem cell differentiation is regulated by PI3K/Tor signaling in response to local cues. Development, 2016. 143(21): p. 3914–3925. [PubMed: 27633989]
55. Miron M, Lasko P, and Sonenberg N, Signaling from Akt to FRAP/TOR targets both 4E-BP and S6K in Drosophila melanogaster. Mol Cell Biol, 2003. 23(24): p. 9117–26. [PubMed: 14645523]
56. Gonczy P and DiNardo S, The germ line regulates somatic cyst cell proliferation and fate during Drosophila spermatogenesis. Development, 1996. 122(8): p. 2437–47. [PubMed: 8756289]
57. Fairchild MJ, Islam F, and Tanentzapf G, Identification of genetic networks that act in the somatic cells of the testis to mediate the developmental program of spermatogenesis. PLoS Genet, 2017. 13(9): p. e1007026. [PubMed: 28957323]
58. Papagiannouli F, The internal structure of embryonic gonads and testis development in Drosophila melanogaster requires scrib, lgl and dlg activity in the soma. Int J Dev Biol, 2013. 57(1): p. 25–34. [PubMed: 23585349]
59. Papagiannouli F, Berry CW, and Fuller MT, The Dlg Module and Clathrin-Mediated Endocytosis Regulate EGFR Signaling and Cyst Cell-Germline Coordination in the Drosophila Testis. Stem Cell Reports, 2019. 12(5): p. 1024–1040. [PubMed: 31006632]
60. Papagiannouli F and Mechler BM, discs large regulates somatic cyst cell survival and expansion in Drosophila testis. Cell Res, 2009. 19(10): p. 1139–49. [PubMed: 19546890]

Highlights: Johnson and Leatherman

- *Merlin* and *expanded* both function to inhibit overproliferation of CySCs in the *Drosophila* testis.
- MAPK/ERK signaling is increased in *Merlin* loss of function mutant *Drosophila* testes.
- MAPK/ERK and Tor signaling is attenuated when *Merlin* is constitutively activated in *Drosophila* testes.
- Regulation of Merlin via phosphorylation provides a mechanism whereby dynamic regulation of signaling in a stem cell population can be achieved.

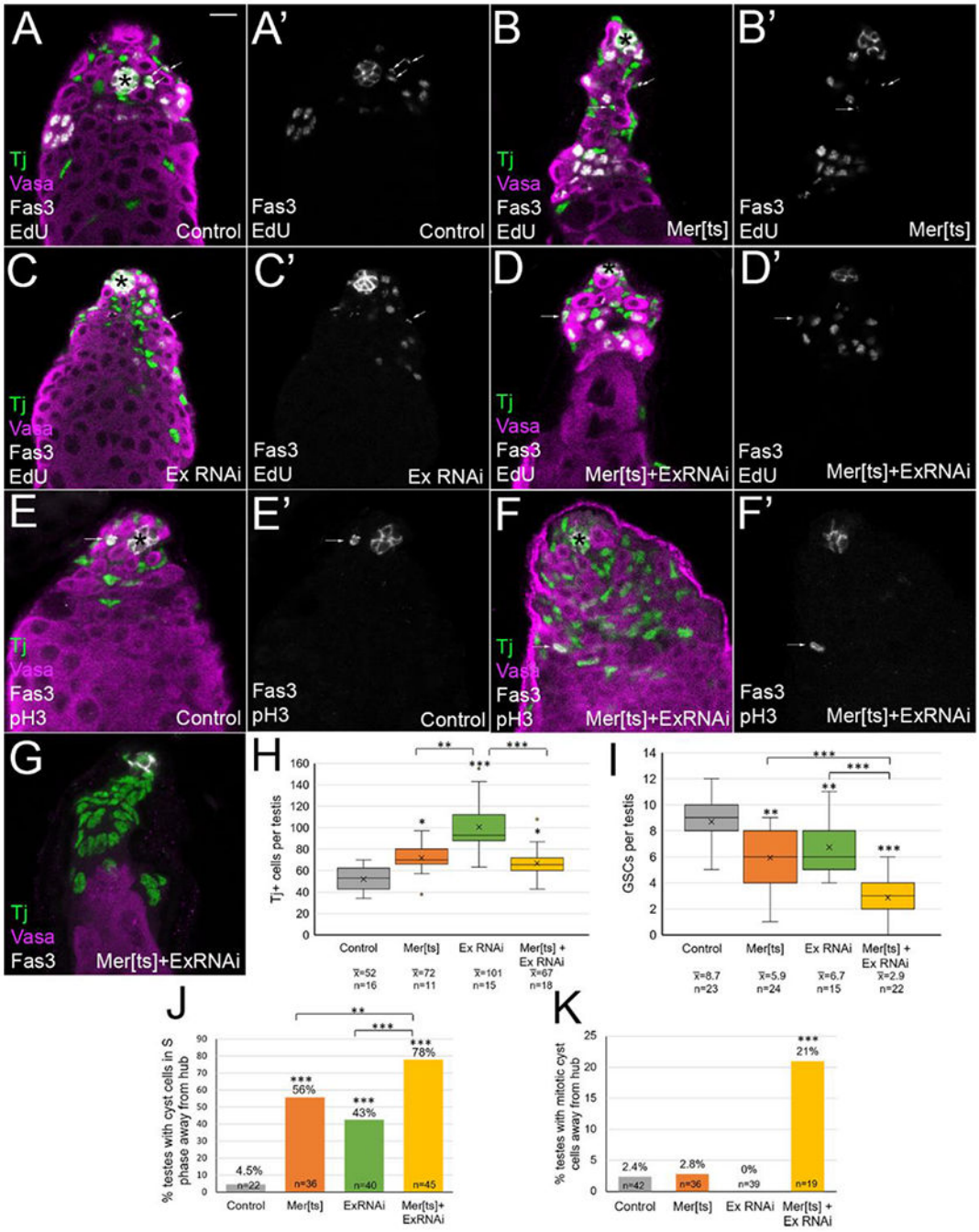

Figure 1:

Merlin and *expanded* depletion caused an increase in cyst lineage cells, a decrease in GSCs, and cyst cells cycled outside of the niche. (A-G) Tj (green) marks cyst lineage cells, vasa (magenta) marks germline cells, fas3 (white) and asterisks mark the hub, EdU (A-D, white) marks cells in S phase, and pH3 (E-F, white) marks cells in mitosis. Testes aged at 29° for 7 days. Bar in A = 10 uM. (A, A') Control testis (FM7; CyO/+; UAS ExRNAi/+), EdU and fas3 alone in A' show cyst lineage cells in S phase were only found adjacent to the hub (arrows). (B, B') *Merlin* ablated testis (Mer[ts]; CyO; UAS ExRNAi/+), (C, C') *expanded*

ablated testis (FM7; TjGal4/+; UAS ExRNAi), and (D, D') double mutant testes (Mer[ts]; TjGal4/+; UAS ExRNAi/+) all showed an increase in Tj+ cells and a decrease in GSCs. Occasional cyst cells in S phase were found away from the hub (arrows, B', C', D'). (E) In control testes (FM7; CyO/+; ExRNAi/+), mitotic cyst lineage cells were found only adjacent to the hub (E, E', arrow). (F) Double mutant testes (Mer[ts]; TjGal4/+; UAS ExRNAi/+) showed rare pH3+ mitotic cyst cells away from the hub (F, F', arrow). (G) Some double mutant testes completely lost their GSCs. (H) Quantitation of Tj+ cells. Box and whisker plot shows the second and third data quartiles in the box divided by a line for the median, and an X for the mean. Whiskers show the extent of the first and fourth quartiles, and dots indicate the location of outlier data points. Single and double mutants all showed a statistically significant increase in Tj+ cells compared to control (FM6; CyO/+; ExRNAi/+). ExRNAi testes showed an increase in Tj+ cells that was statistically higher than either Mer[ts] or Mer[ts]+ExRNAi conditions. (I) Quantitation of GSCs. Single and double mutants all showed a statistically significant decrease in GSC number compared to controls. Double mutant showed a larger decrease in GSC number than either single mutant alone. (J) Quantitation of percent of testes with at least one cyst cell in S phase more than two germ cell diameters away from the hub. Double mutant condition showed greater fraction of testes with this phenotype present. (K) Quantitation of percent of testes with at least one cyst cell in mitosis away from the hub. Control and single mutants show negligible numbers, but double mutants showed a statistically significant fraction of testes with this phenotype. Statistical significance determined by one-way Anova followed by Tukey Kramer post hoc test for H and I, and chi square goodness of fit statistical test for J and K, with *$p<0.05$, **$p<0.01$, ***$p<0.001$.

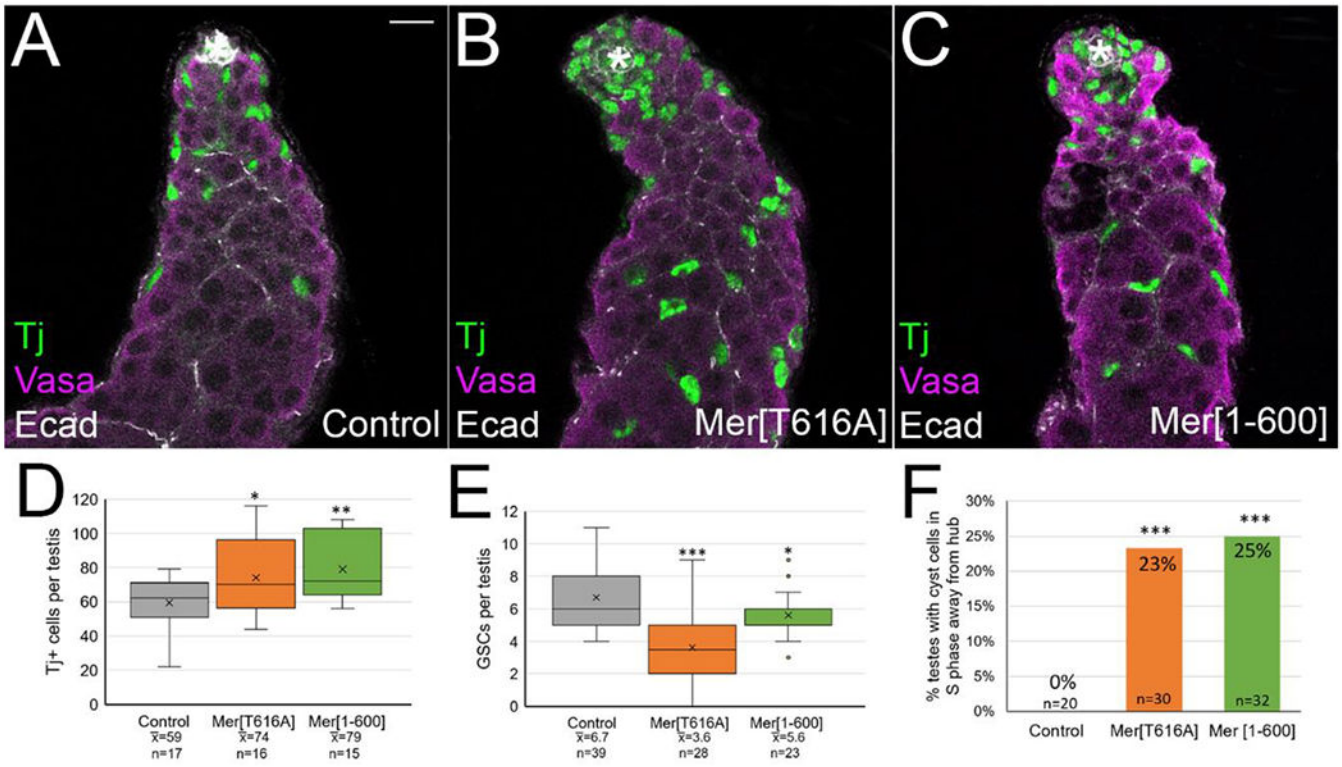

Figure 2:

Constitutive Merlin caused accumulation of excess cyst lineage cells, decreased GSCs, and cyst cells cycled outside of the niche. (A-C) Tj (green) shows cyst lineage cells, vasa (magenta) shows germ cells, Ecadherin (white) shows hub and cyst cell membranes. Asterisk marks hub. Bar in A = 10 uM. Testes aged at 29° for 12 days. Expression of constitutive *Merlin* in the cyst lineage (*c587 Gal4; UAS Mer[T616A]/+* in B, and *c587 Gal4; UAS Mer[1-600]/+* in C) led to more Tj-positive cells and fewer GSCs per testis than controls (A, *c587 Gal4).* (D) Quantitation showed constitutive *Mer* testes had a significant increase in the average number of Tj+ cells per testis compared to controls. The percent increase in Tj+ cells over controls were 25% and 34% for the two constitutive lines respectively (compare to 39% over controls observed with *Merlin* loss of function in Figure 1H). (E) Quantitation showed that constitutive *Mer* testes had a significant decrease in the average number of GSCs per testis compared to controls. Statistical significance determined by one-way Anova followed by Tukey Kramer post hoc test, ***p<0.001, **p<0.01, *p<0.05. (F) Quantitation showed that many constitutive *Mer* testes had at least one EdU-positive cyst cell greater than two germ cell diameters from the hub, a phenotype not observed in controls. Statistical significance determined by chi square goodness of fit statistical test. Testis images with examples of cells in S phase away from hub shown in Supplemental Figure 2.

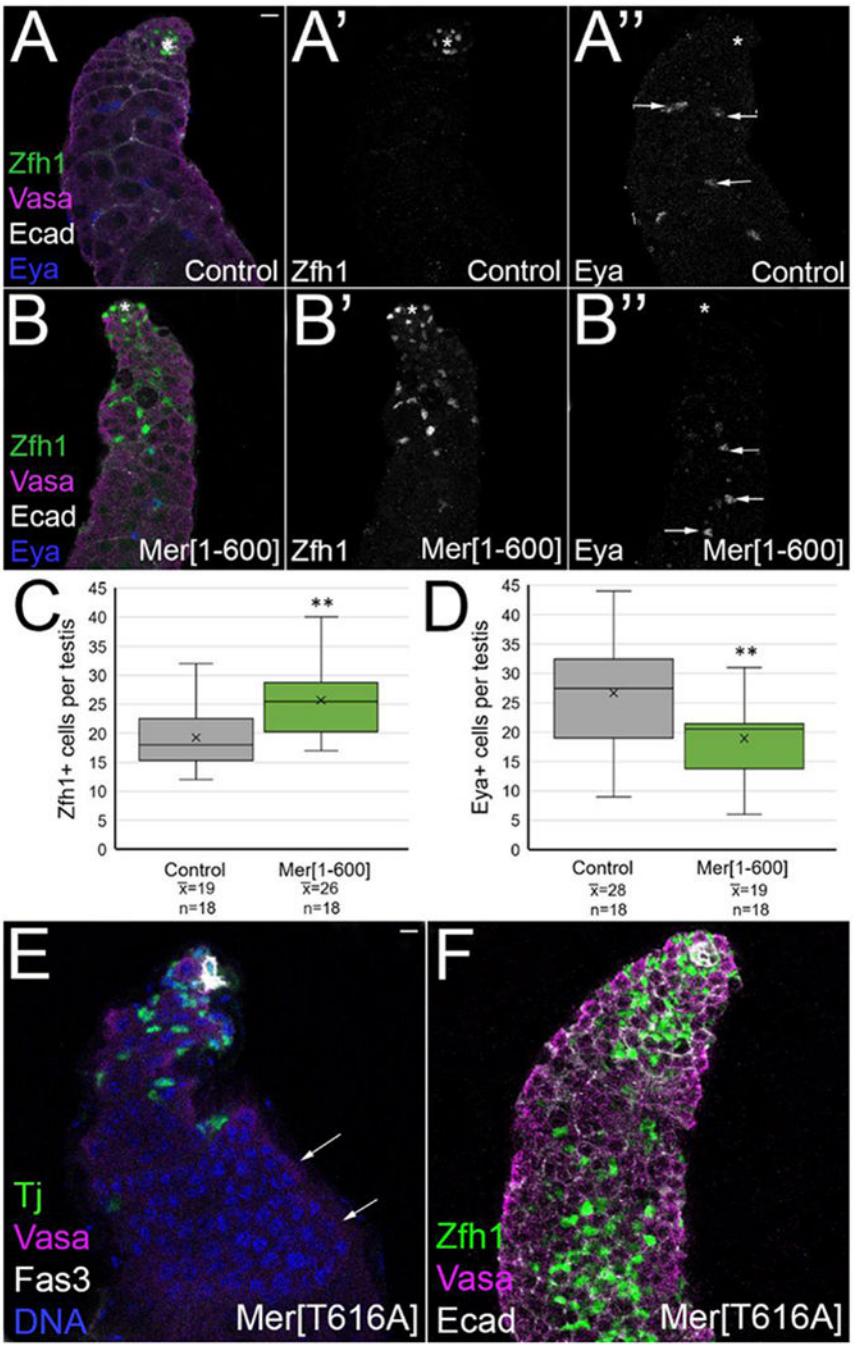

Figure 3:

Constitutive Merlin led to an increase in Zfh1-positive cells, and these cells accumulate away from the hub. (A, B, E, F) Zfh1 (green in A, B, F) marks CySCs, Tj (green in E) marks cyst lineage cells, vasa (magenta) marks germ cells, Ecadherin (white in A, B, F) marks hub and cyst cell membranes, Fas3 (white in E) marks hub, Eya (blue in A, B) marks differentiating cyst cells. (A', B') Zfh1 alone (white). (A", B") Eya alone (white). Hub marked with an asterisk. Bars in A and E = 10 uM. Testes aged 14 days at 29°. (A-A") Control testes *(c587 Gal4)* showed Zfh1-bright cells only adjacent to hub, while Eya-bright

cyst cells (A”, arrows) were found associated with late spermatogonia and spermatocyte germline cysts. (B-B”) Testes with constitutive Merlin (*c587 Gal4; UAS Mer[1-600]*) accumulated excess Zfh1-bright cells away from the hub (B’), while Eya-bright cells were found further from the hub (B”, arrows). A similar result was found with *Mer[T616A]* (data not shown). (C) Quantitation showed that constitutive *Mer* caused an increase in the average number of Zfh1 cells per testis compared to control. (D) Quantitation showed that constitutive *Mer* caused a reduction in the average number of Eya-bright cells per testes. Statistical significance by Student t-test. **p<0.01. (E) Some constitutive *Mer* testes (c587 Gal4; UAS *MerT515A/+)* accumulated spermatogonial cysts greater than 16 cells (arrows), a phenotype never observed in control testes. Spermatogonia are identified as vasa+ DNA-bright cells. (F) Rare testes with constitutive *Mer* accumulated Zfh1+ cells throughout the testis, accompanied by GSC-like cells (identified as small vasa+ cells found as individual germ cells, not in spermatogonial cysts).

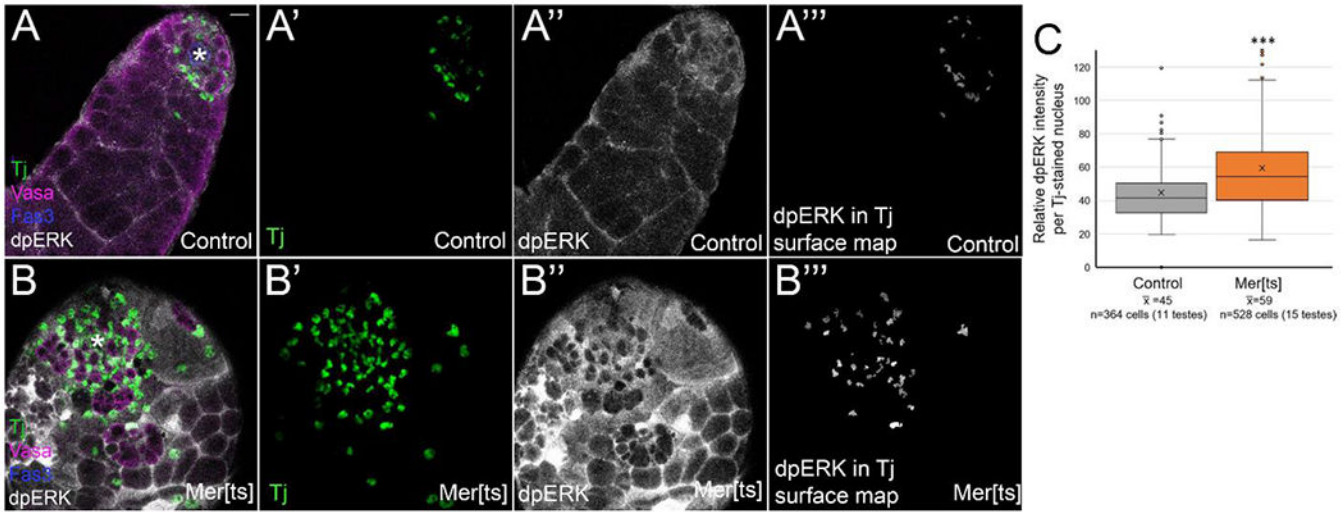

Figure 4:

Cyst lineage cells in *Merlin* loss of function testes accumulated higher levels of dpERK than controls. (A,B) Tj (green) marks cyst lineage cell nuclei, vasa (magenta) marks germ cells, fas3 (blue) and asterisk mark hub, and dpERK stain (white) shows location of MAPK signaling. (A', B') Tj (green). (A", B") dpERK (white). (A"',B"') 3D surface map of Tj stain was generated in Image J, and dpERK staining is shown only within those cyst lineage nuclei. Bar in A = 10 uM. (A-A"') Control testes *(FM7)* showed dpERK accumulation in nuclei and cytoplasm of cyst lineage cells. (B-B"') *Mer[ts]* testes showed an increase in the number of Tj+ cells compared to control (B'), and an increase in dpERK accumulation (B"). (C) Quantitation of dpERK intensity, limited to area of Tj nuclei. Relative dpERK staining intensity was measured in each cyst lineage cell nucleus using the 3D surface map of the Tj stain. The average dpERK intensity per cell is shown (n=394 cells for control, 530 cells for *Mer[ts]*). Statistical analysis performed using Student t-test. ***p<0.001. Statistical significance (p<0.05) was also achieved when individual cell intensities within a testis were averaged, and each testis was treated as one n value.

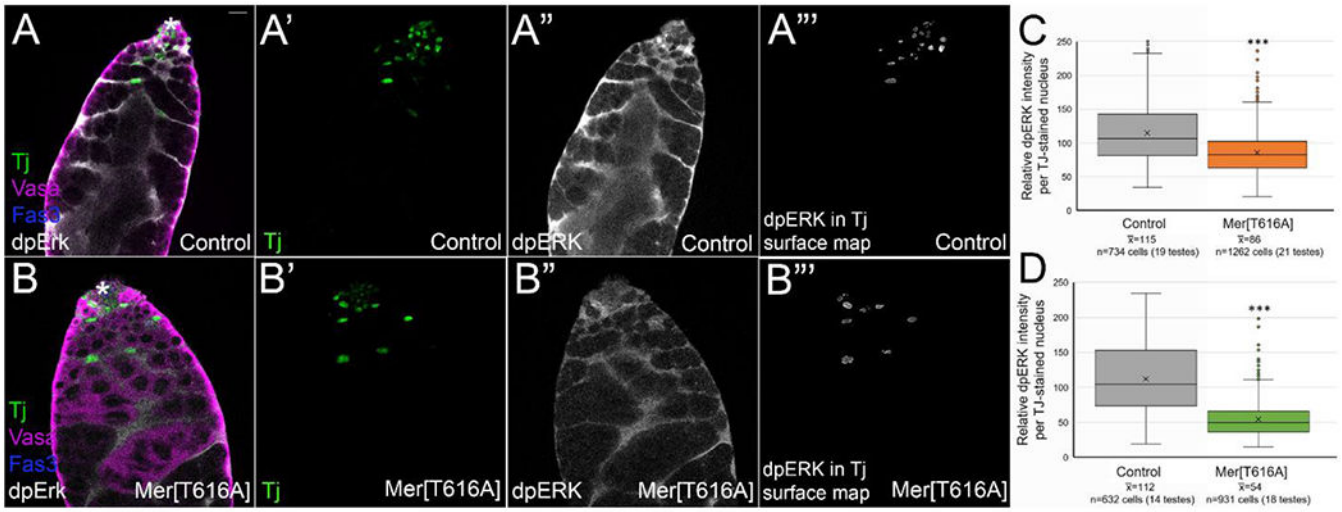

Figure 5:

Cyst lineage cells with constitutive *Merlin* accumulated lower levels of dpERK than controls. (A,B) Tj (green) marks cyst lineage cell nuclei, vasa (magenta) marks germ cells, fas3 (blue) and asterisk mark hub, and dpERK (white) shows location of MAPK signaling. (A', B') Tj (green). (A", B") dpERK (white). (A"',B"') 3D surface map of Tj stain was generated in Image J, and dpERK staining is shown only within those cyst lineage nuclei. Bar in A = 10 uM. (A-A"') Control testes *(c587 Gal4)* showed dpERK accumulation in nuclei and cytoplasm of cyst lineage cells. (B-B"') c587 Gal4; UAS Mer^{T616A} testes showed a reduced accumulation of dpERK (B") compared to control (A"). (C, D) Quantitation of dpERK in c587 Gal4; UAS *Mer[T616A]* and c587 Gal4; UAS *Mer[1-600]* testes compared to their stain-matched controls (relative dpERK staining intensity was measured in each nucleus using the 3D surface map of the Tj stain) showed significant reduction in average dpERK accumulation with constitutive *Mer* compared to controls. ***$p<0.001$ by Student t-test. Statistical significance ($p<0.01$ and $p<0.001$ for *Mer[T616A]* and *Mer[1-600]* respectively) was also achieved when individual cell intensities within a testis were averaged, and each testis was treated as one n value.

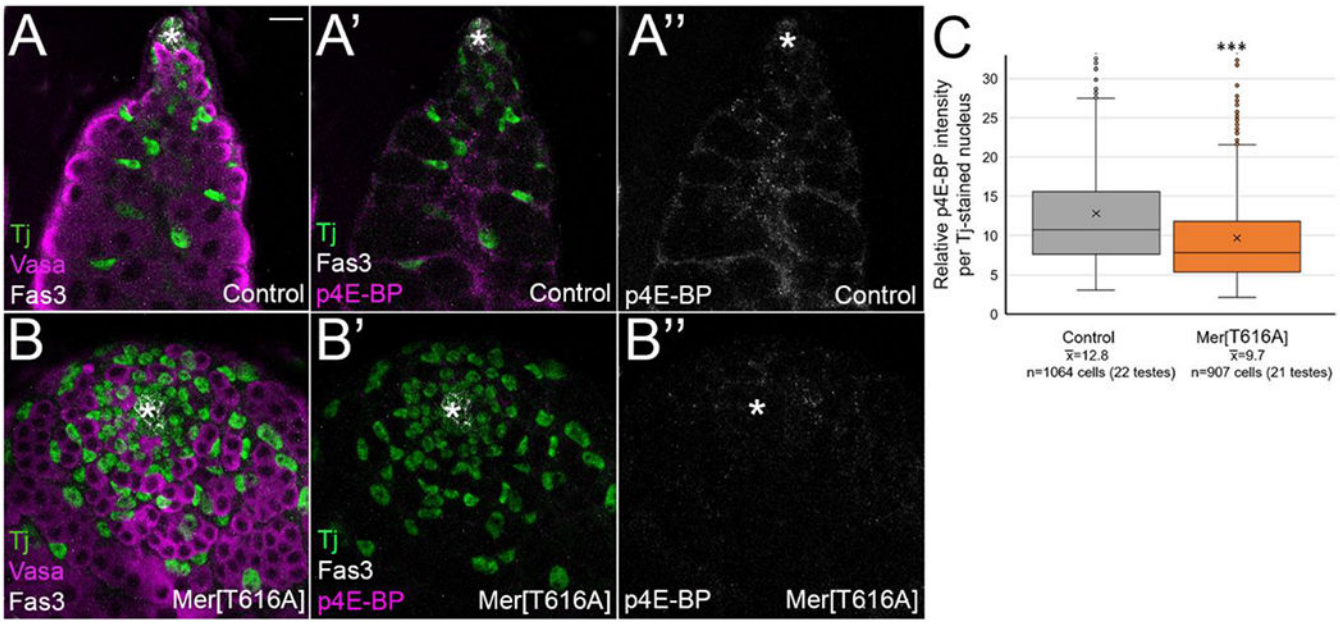

Figure 6:

Constitutive *Merlin* in the cyst lineage repressed PI3K/Tor signaling, as shown by phosphorylation of the Tor direct target 4E-BP1. (A, A',B, B') Tj (green) shows cyst lineage cells, (A, B) Vasa (magenta) shows germ cells, and Fas3 (white, A, A', B, B') or asterisk shows hub. p4E-BP (magenta in A'and B', white in A" and B") is a direct target of Tor phorphorylation. Bar = 10 uM. (A-A") Control testes (c587 Gal4) showed p4E-BP accumulation in cytoplasm and nucleus of cyst lineage cells. (B-B") Constitutive *Merlin* (c587 Gal4; UAS *Mer[T616A]*) showed reduction in p4E-BP stain intensity, indicating that active Merlin represses Tor signaling. (C) Quantitation of average p4E-BP staining intensity in c587 Gal4; UAS *Mer[T616A]* compared to their stain-matched c587 Gal4 controls (relative p4E-BP staining intensity was measured in each nucleus using the 3D surface map of the Tj stain) showed a significant reduction on p4E-BP stain intensity with constitutive *Mer* compared to controls. ***p<0.001 by Student t-test. Statistical significance (p<0.05) was also achieved when individual cell intensities within a testis were averaged, and each testis was treated as one n value.

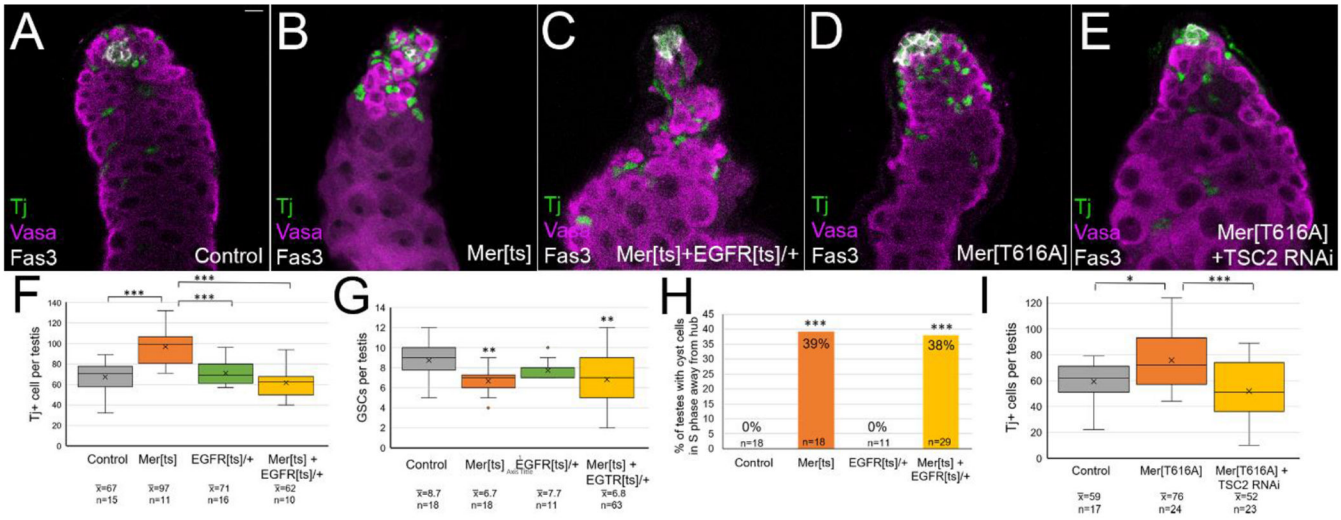

Figure 7:

Modulation of EGFR and Tor signaling rescued some aspects of the *Merlin* gain and loss of function phenotypes. (A-E) Tj (green) shows cyst lineage cells, Vasa (magenta) shows germ cells, Fas3 (white) shows hub. (A-C) Testes aged at 29° for 8 days. (D-E) Testes aged at 29° for 7 days. (A) Control testes (*FM7; CyO/+*) (B) *Mer* mutant testes (*Mer[ts]; CyO/+*) showed increased number of Tj cells compared to control. (C) EGFR heterozygosity in *Mer* mutant testes (Mer[ts]; EGFR[ts]/+) showed rescue of Tj cells back to control levels. (D) Expression of constitutive *Merlin* (*c587 Gal4; UAS Mer[T616A]*) caused excess Tj+ cells to accumulate. (H) Expression of a TSC2 RNAi transgene together with *Mer[T616A]* rescued the increase in Tj+ cells observed with *Mer[T616A]* alone. (F) Quantitation showed that EGFR heterozygosity rescued the increase in Tj cells observed with Mer[ts] back to control levels. (G) Quantitation showed that EGFR heterozygosity did not rescue the decrease in GSCs observed with Mer[ts]. (H) Quantitation showed that EGFR heterozygosity did not rescue the phenotype of cyst cells entering S phase away from the hub observed with Mer[ts]. (I) Quantitation showed TSC2 RNAi rescued the increase in Tj cells observed with Mer[T616A] expression. Statistical significance determined by one-way Anova followed by Tukey Kramer post hoc test in F, G, and I. Statistical significance determined by chi square goodness of fit test in H. ***p<0.001, **p<0.01, *p<0.05.

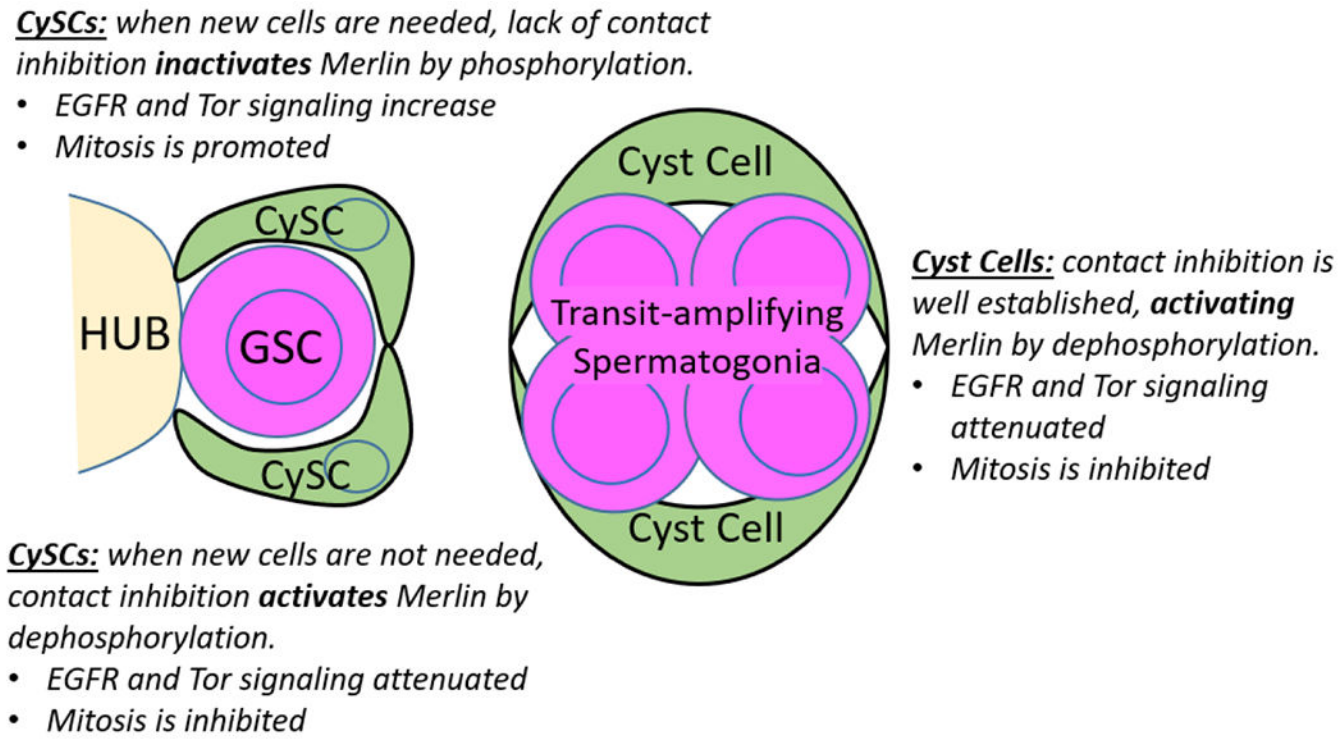

Figure 8:

Model for Merlin activity. CySCs respond to local conditions, modulating Merlin activity to dynamically regulate mitosis and signaling. Differentiating cyst cells activate Merlin to inhibit mitosis and attenuate EGFR signaling to accomplish spermatogonial transit amplification.